

Does the interaction potential determine both the fragility of a liquid and the vibrational properties of its glassy state ?

Patrice Bordat, Frédéric Affouard, Marc Descamps*
*Laboratoire de Dynamique et Structure des Matériaux Moléculaires
UMR 8024, Université Lille I, 59655 Villeneuve d'Ascq cedex, France*

K. L. Ngai
Naval Research Laboratory, Washington, DC 20375-5320, USA
(Dated: November 25, 2018)

By performing molecular dynamics simulations of binary Lennard-Jones systems with three different potentials, we show that increase of anharmonicity and capacity for intermolecular coupling of the potential is the cause of (i) the increase of kinetic fragility and nonexponentiality in the liquid state, (ii) the T_g -scaled temperature dependence of the nonergodicity parameter determined by the vibrations at low temperatures in the glassy state. Naturally these parameters correlate with each other, as observed experimentally by T. Scopigno *et al.*, Science **302**, 849 (2003).

PACS numbers: 61.20.Ja, 64.60.Ht, 64.70.Pf

The structural relaxation time, τ , of all glass-forming liquids increases on cooling. It becomes so long at some temperature T_g that equilibrium cannot be maintained and the liquid is transformed to a glass. T_g is defined as the temperature at which τ reaches some arbitrarily chosen long time, say 10^2 s. Although this behavior is shared by glass-formers of diverse chemical and physical structures, the scaled temperature dependence of τ in the liquid state can differ greatly from one liquid to another in the degree of departure from the Arrhenius scaled temperature dependence [1, 2]. The departure can be characterized by the rapidity of the change of $\log(\tau)$ with T_g/T at $T_g/T=1$, which is given by the steepness index or the fragility m defined by [3]

$$m = \left. \frac{d \log(\tau)}{d(T_g/T)} \right|_{T_g/T=1}. \quad (1)$$

The values of m of glass-formers of all kinds vary over a large range, from the least value of about 17 for strong glass-formers (like silica) having nearly Arrhenius scaled temperature dependence of τ , to values as high as about 200 found for some glass-formers called fragile. Naturally, such large variations observed in m beg the question of its microscopic origin. Several attempts have been made in the past to correlate m with other dynamic or thermodynamic properties, with the hope that the correlations will lead to the factor or factors that determine m . Examples include: (1) The correlation of m with $n \equiv (1 - \beta)$ at $T = T_g$, where β is the stretched exponent in the Kohlrausch function, $\exp[-(t/\tau)^\beta]$, used to fit the time dependence of the correlation functions such as the intermediate scattering functions. (2) The correlation of m or $(1 - \beta)$ with the mean square displacement $\langle u^2 \rangle$ obtained [4] from quasielastic neu-

tron scattering measurement of the Debye-Waller factor $\exp[-\langle u^2 \rangle Q^2/3]$. Glass-former with larger m or $(1 - \beta)$ has a larger $\langle u^2 \rangle$ at the same value of T/T_g and rise more rapidly as a function of T/T_g , below T_g as well as near and across T_g in the liquid states [4]. (3) The correlation between m and the slope of the change of the configurational entropy, S_c , with T/T_g at T_g [5]. (4) The correlation of m with the statistics of potential energy minima of the energy landscape [6, 7]. (5) The correlation of m with the temperature dependence of the shear modulus of the liquid [8]. Perhaps the most intriguing of all correlations is (6) between m and the vibrational properties of the glass at temperatures well below T_g found recently by T. Scopigno *et al.* [9]. The nonergodicity parameter, $f(Q, T)$, at $Q=2 \text{ nm}^{-1}$ at very low temperatures is determined by vibrations. From inelastic X-ray scattering data, its temperature dependence is well described by $[1 + \alpha (T/T_g)]^{-1}$. T. Scopigno showed that m and α are proportional for many glass-formers. Apparently, this last correlation (6) seems to be related to (2) for $\langle u^2(T/T_g) \rangle$ from neutron scattering at temperatures well below T_g .

In any glass-former, it is the interaction potential, $V(r)$, that determines ultimately all dynamic, thermodynamic and vibrational properties at all temperatures, below and above T_g . Changes in any of quantities, m , n , $\langle u^2(T/T_g) \rangle$, α , S_c , free volume ν [10] and the degree of dynamic heterogeneity, from one glass-former to another originate from the change in $V(r)$. Thus, correlations found between these quantities are clues for finding out which aspects of $V(r)$ determine them and give rise to the correlations between them. One would like to examine the interaction potentials in real glass-formers. However, in such materials, the different kinds of chemical bonding and the different sizes of the basic structural unit make the comparisons ambiguous. For this reason we consider the binary Lennard-Jones particles with different choices of interaction potentials $V(r)$ between the particles, and perform molecular dynamics (MD) simulations on them

*Electronic address: bordat@cyano.univ-lille1.fr

to obtain m , n , α , and $\langle u^2(T/T_g) \rangle$. Correlations are found between all these quantities, thus reproducing the empirical findings from real glass-formers. Since the number of particles as well as their density are the same, the changes of these quantities are predominantly due to the change in $V(r)$. The latter is well controlled, and therefore we identify anharmonicity and the capacity of intermolecular coupling of $V(r)$ to be responsible for enhancement of m , n , α , and $\langle u^2(T/T_g) \rangle$, and hence their correlations.

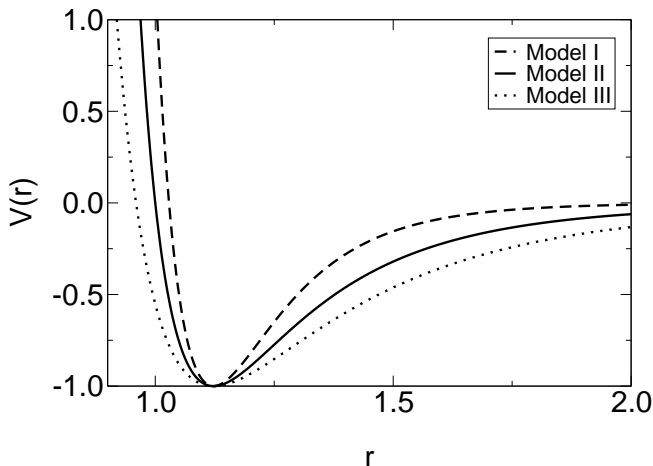


FIG. 1: Potential $V(r)$ governing the A-A interaction. The dashed curve is the (8,5) LJ potential for model I, the solid curve is the (12,6) LJ potential for model II and the dotted curve is the (12,11) LJ potential for model III.

MD simulations were performed on binary Lennard-Jones (LJ) particles systems with three different interaction potentials by the MD package DLPOLY [11]. Technical details of the MD simulations are given in [12]. We have performed from 10^5 to 6×10^7 time steps, depending on temperature. We have investigated 12 temperatures in the range of $[0.675 - 5]$, $[0.416 - 5]$ and $[0.26 - 2]$ for Model I, II and III respectively. All models are composed of 1500 uncharged particles (1200 species A and 300 species B). The generalized (q, p) LJ potentials have the form, $V(r) = \frac{E_0}{(q-p)} \left(p \left(\frac{r_0}{r} \right)^q - q \left(\frac{r_0}{r} \right)^p \right)$. The parameters r_0 and E_0 represent the position of the minimum of the well and its depth, respectively. The reduced LJ units [13] are used. The choice of $q=12$ and $p=6$ corresponds to the standard LJ potential used by Kob & Andersen (K-A) [14] and others for extensive studies by simulation. For the purpose of investigating the change of dynamics with controlled change of $V(r)$, we developed two other models by changing only the exponents, q and p , of the LJ potential for the A - A interactions. They are $(q=8, p=5)$ and $(q=12, p=11)$ and shown together with the (12,6) LJ potential in Fig. 1. The well depth and the position of the minimum of $V(r)$ are unchanged, and we have kept the standard (12,6) LJ potentials of the K-A

model for the A - B and B - B interactions, in order to retain as much as possible the remarkable ability of the K-A model to form a glass upon cooling. The (12,11) LJ potential is more harmonic than the classical (12,6) LJ potential, while the (8,5) LJ potential is a flat well and exceedingly anharmonic. Whenceforth the (12,11), (12,6) and (8,5) potentials are referred to as Model I, II and III respectively, reminding us that anharmonicity is increasing in this order.

The structure has been briefly studied by the radial distribution functions $g(r)$ of the (12,11) and (8,5) models, which have been calculated and found very similar to that of (12,6) model in the temperature ranges investigated. Respectively for models I, II and III, the position of the first peak of $g(r)$ is at 1.072, 1.066 and 1.057 and its width at half the maximum is 0.129, 0.147 and 0.191. The $g(r)$ of the three models in the supercooled state is similar to that in the liquid regime, ensuring the structures have disorder in the mid- and long-range.

Dynamics have been investigated by computing the self $F_S(Q, t)$ and the total $F(Q, t)$ intermediate scattering functions of particles A at $Q_0 = 2\pi/r_0$ for the three models. At high temperatures, $F_S(Q_0, t)$ decays linear exponentially to zero with a characteristic time of about 0.45 close to crossover time $t_c \approx 1$ to 2 ps used as a fundamental time in the Coupling Model (CM) [15, 16]. When temperature is lowered, the dynamics slows down dramatically and a two-step process appears. This behavior is well described by the Mode Coupling Theory (MCT) [17]. From the $F_S(Q_0, t)$ at each of these lower temperatures, we determine the nonergodicity parameter (height of the plateau), $f_S(Q_0, T)$, the relaxation time, τ_A , and the stretched exponent, β , from the fit to the second step decay of $F_S(Q_0, t)$ by $f_S(Q_0, T) \exp[-(t/\tau_A)^\beta]$. Shown in Fig. 2 are $F_S(Q_0, t)$ versus t/τ_A of all three models at the reference temperature T_{ref} defined by $\tau_A(T_{ref}) = 46435.8$, a very long time in our simulations. The values of T_{ref} are 0.688, 0.431 and 0.263 for Models I, II and III respectively.

Shown in Fig. 2 (inset) are β of the three models as a function of T_{ref}/T . At any T_{ref}/T , $(1 - \beta)$ is least for model I and largest for model III. At $T = T_{ref}$, $\beta = 0.69$, 0.65 and 0.60 respectively for Models I, II and III. Thus $(1 - \beta)$ increases with anharmonicity. In Fig. 3, $\log(\tau_A)$ is plotted against T_{ref}/T and the data of the three models show systematic change. It can be seen that the slope, fragility index $m(\tau_A) \equiv \frac{d \log(\tau_A)}{d(T_{ref}/T)}$ as $(T_{ref}/T) \rightarrow 1$, increases monotonically in the order of Models I, II and III. The values of $m(\tau_A)$ determined from this latter relation are 15.07, 18.57 and 26.58 for Models I, II and III. Alternatively, the estimated values of $m(\tau_A)$ based on Sastry's method [7] are 0.195, 0.241 and 0.405 for Models I, II and III, respectively. Hence, $m(\tau_A)$ increases with anharmonicity. The fragility index found in the present study for model II is in good agreement with the value determined in an earlier work on the same model [7]. The diffusion coefficient, D_A , of particles A was calculated from the mean-square displacement $\langle u^2(t) \rangle$ at

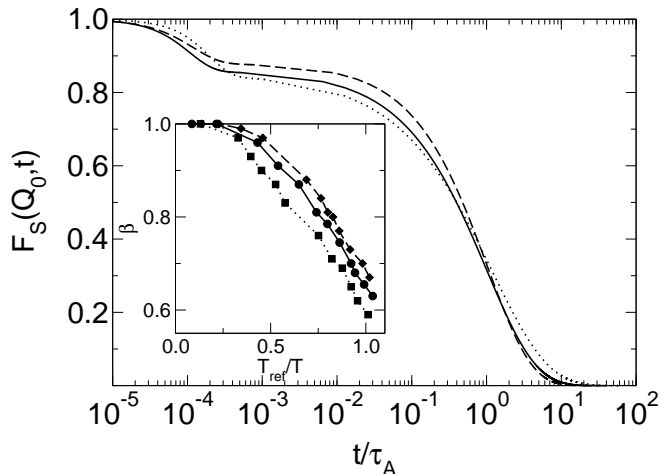


FIG. 2: Self intermediate scattering function $F_S(Q_0, t)$ versus scaled time t/τ_A . Dashed, continuous and dotted lines are for Models I, II and III respectively. For all three models, $\tau_A(T_{ref}) = 46435.8$. The inset shows the stretched exponent $\beta = (1 - n)$ as a function of the scaled reciprocal temperature T_{ref}'/T for the three models. (\blacklozenge) Model I, (\bullet) Model II and (\blacksquare) Model III. For definitions of τ_A and β , see text.

long times when $\langle u^2(t) \rangle$ assumes the linear t dependence. Here another T'_{ref} is defined as the temperature at which D_A is equal to 1.86×10^{-5} . In the inset of Fig. 3, we plot $\log(1/D_A)$ against T'_{ref}/T for each of the three models. They exhibit the same pattern as $\log(\tau_A)$. Again the steepness or fragility index, $m(D_A) \equiv \frac{d \log(1/D_A)}{d(T'_{ref}/T)}$ as $(T'_{ref}/T) \rightarrow 1$, increases monotonically in the order of Models I, II and III, or with anharmonicity.

So far we are concerned for dynamic quantities and their correlations for $T > T_{ref}$, as analogues of them in the liquid state of real glass-formers. Next we examine the vibrational properties of the three models at temperatures lower and much lower than T_{ref} . At low temperatures, relaxation of any kind is absent in the simulation time window, and the nonergodicity parameter $f(Q, T)$ determined from $F(Q, t)$ is contributed entirely from vibrations. As performed in [9], we have followed the behaviour of $f(Q \rightarrow 0, T)$ which has been obtained by a Q-quadratic extrapolation of $f(Q, T)$ for the lowest temperatures. The results of the three models are shown by a plot of $f(Q \rightarrow 0, T)^{-1}$ versus T/T_{ref} in Fig. 4.

In all three cases, the dependence of $f(Q, T)^{-1}$ on T/T_{ref} is approximately linear, and $f(Q, T)^{-1}$ has the extrapolated value of unity at the origin. The dependence of $f(Q, T)$ from simulation on T/T_{ref} is governed by the parameter, α , through the expression,

$$f(Q, T)^{-1} = 1 + \alpha \frac{T}{T_{ref}}, \quad (2)$$

just like a similar expression used to represent the dependence of $f(Q, T)$ on T/T_g of real glass-formers obtained

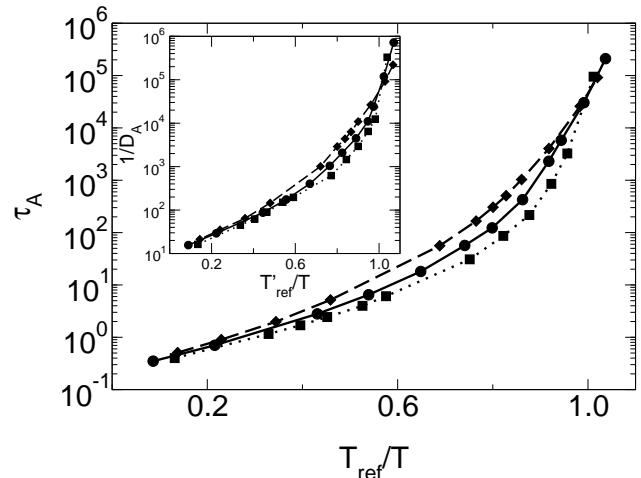


FIG. 3: The relaxation times τ_A obtained from $F_S(Q_0, t)$ for the three models as a function of T_{ref}'/T where T_{ref}' is defined as the temperature at which τ_A reaches 46435.8. (\blacklozenge) Model I, (\bullet) Model II and (\blacksquare) Model III. T_{ref}' is the analogue of T_g for simulations when the dynamics of the system slows down to more than 10 ns. In the inset, the reciprocal of diffusivity D_A of A particles for the three models are given as a function of T'_{ref}/T . Here T'_{ref} is now defined as the temperature at which D_A is equal to 1.857432×10^{-5} .

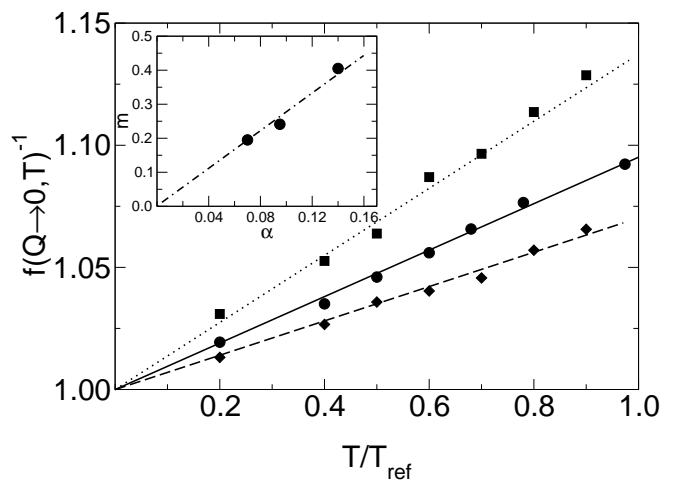


FIG. 4: $f(Q, T)^{-1}$ versus T/T_{ref} for the three models. (\blacklozenge) Model I, (\bullet) Model II and (\blacksquare) Model III. $f(Q, T)^{-1}$ is almost linear relative to T/T_{ref} with a slope noted α . The inset shows the correlation of the fragility m with α from the results of the three models.

by inelastic X-ray scattering [9]. We see from Fig. 4 that the increase of $f(Q, T)^{-1}$ with T/T_{ref} is fastest for model III and slowest for model I. Equivalently stated, the slope α is largest for model III and smallest for model I. α increases with anharmonicity of the potential, like $m(\tau_A)$ or $m(D_A)$, and $(1 - \beta)$, as seen before (Figs. 1, 2, 3). Hence

the interacting potential is the origin of the correlation of α with $m(\tau_A)$ or $m(D_A)$, and $(1 - \beta)$ in our simulation, suggesting the same holds for real glass-formers. Moreover, in the inset of Fig. 4, we observe that $m(\tau_A)$ and α are proportional together as shown in [9].

Presumably there is no disagreement that the interaction potential is pivotal in determining all dynamic, thermodynamic and vibrational properties of glass-formers at all temperatures. With all these experimentally accessible properties originating from the interaction potential, it is not surprising to find correlations or anticorrelations between them. Making this point is one of the motivations of the work in demonstrating that the various correlations between α , m , $(1 - \beta)$ and $\langle u^2(T/T_g) \rangle$ observed in real glass-formers are reproduced by simulations as the analogues of correlations between α , $m(\tau_A)$, $m(D_A)$ and $(1 - \beta)$ by varying the interaction potential $V(r)$. The results confer a bonus in identifying which feature of the interaction potential is responsible for enhancement of α , $m(\tau_A)$, $m(D_A)$ and $(1 - \beta)$. Certainly the anharmonicity of $V(r)$ increases when going from Model I to II and III, but one also can observe from Fig. 1 that the energy barrier becomes lower and flatter. The latter trend means that neighboring LJ particles are more coupled in their motions. The increase in interparticle coupling from Model I to Model III is consistent with the position of the first peak of radial distribution functions $g(r)$ (1.072, 1.066 and 1.057 for Models I, II and III respectively) and with its width at half the maximum (0.129, 0.147 and 0.191 for Models I, II and III). This insight from simulation, when transferred to real glass-formers, suggests that the capacity for intermolecular coupling and anharmonicity of the interaction potential determine the dynamic, thermodynamic and vibrational properties of glass-formers above as well as below T_g . Although the thermodynamic variables, configurational entropy S_c and free volume ν , are determined by $V(r)$, they reenter into the dynamics by their influence on molecular mobility. Thus two factors govern dynamics, the capacity for intermolecular coupling directly from $V(r)$, and S_c and ν that come indirectly through $V(r)$. On supercooling a liquid, S_c and ν change, and since the kinetic fragility m is the slope of T_g -scaled temperature variation of τ , it is unsurprising that m is correlated with the slope of the corresponding change of S_c , i.e., the thermodynamic fragility. The capacity for intermolecular coupling of $V(r)$ is solely responsible for the shape of the

dispersion or the nonexponentiality parameter $(1 - \beta)$, and it also determines τ in conjunction with S_c and ν . The results of our simulation with the three potentials support this view. Increasing the density of the particles of the binary Lennard-Jones system with the fixed (12,6) potential effectively forces the particles to be closer to each other and thereby increases intermolecular coupling. The simulation performed in this manner [7] showing that m increases with density can be reinterpreted as due to increase of intermolecular coupling. Intermolecular coupling manifests itself in the dynamic properties in various ways. The most direct way is the width of the dispersion measured by $(1 - \beta)$. The others include : (1) the $Q^{-2/(1-\beta)}$ dependence of τ obtained by quasielastic neutron scattering [4], and (2) the proportionality [16] between $(1 - \beta)$ and $(\log(\tau) - \log(\tau_\beta))$ at constant $\log(\tau)$ or at T_g (where τ_β is the Johari-Goldstein relaxation time). All these are evidences for intermolecular coupling that must be taken into consideration in conjunction with S_c and ν for explaining all observed experimental facts in the liquid state. At low temperatures and deep in the glassy state, S_c and ν having constant values cannot influence the temperature dependence of the vibrational properties characterized by α . Hence, α is controlled by the anharmonicity of $V(r)$, as demonstrated by the simulations.

In summary, we demonstrate by using three different interparticle potentials of binary Lennard-Jones systems that the capacity for intermolecular coupling and anharmonicity of the potential are responsible for the correlations between various dynamic, thermodynamic and vibrational properties of glass-formers. Increase of the capacity for intermolecular coupling and anharmonicity has the effects of increasing the kinetic fragility, m , and the nonexponentiality parameter, $(1 - \beta)$, in the liquid state, and of increasing in the glassy state the parameter α that characterize the T_g -scaled temperature dependence of the nonergodicity parameter determined by vibrations at low temperatures. The correlations between m , $(1 - \beta)$, α and other quantities follow as consequences, and their observations by experiments explained.

Acknowledgments. — The authors wish to thank for the use of the computational facilities of the IDRIS (Orsay, France) and the CRI (Villeneuve d’Ascq, France). This work was supported by the INTERREG III (FEDER) program (Nord-Pas de Calais/Kent). Work at NRL was supported by the Office of Naval Research.

-
- [1] W. T. Laughlin and D. R. Uhlmann, *J. Phys. Chem.* **76**, 2317 (1972).
 [2] C. A. Angell, *J. Non-Cryst. Solids* **131-133**, 13 (1991).
 [3] D. J. Plazek and K. L. Ngai, *Macromolecules* **24**, 1222 (1991). R. Böhmer and C. A. Angell, *Phys. Rev. B* **45**, 10091 (1992).
 [4] K. L. Ngai, *J. Non-Cryst. Solids* **275**, 7 (2000).
 [5] K. Ito, C. T. Moynihan, and C. A. Angell, *Nature* **398**, 492 (1999).
 [6] R. J. Speedy, *J. Phys. Chem. B* **103**, 4060 (1999).
 [7] S. Sastry, *Nature* **409**, 164 (2001).
 [8] J. Dyre and N. B. Olsen, *cond-mat/0211042* (2003).
 [9] T. Scopigno, G. Ruocco, F. Sette, and G. Monaco, *Science* **302**, 849 (2003).
 [10] K. L. Ngai, L.-R. Bao, A. F. Yee, and C. L. Soles, *Phys. Rev. Lett.* **87**, 215901 (2001).

- [11] W. Smith and T. R. Forester, *The DLPOLY user manual*, CCLRC, Daresbury Laboratory, England (2001).
- [12] P. Bordat, F. Affouard, M. Descamps, and F. Müller-Plathe, *J. Phys.: Cond. Matter* **15**, 5397 (2003).
- [13] M. P. Allen and D. J. Tildesley, eds., *Computer Simulation of Liquids* (Oxford Science, Oxford, 1987).
- [14] W. Kob and H. C. Andersen, *Phys. Rev. E* **51**, 4626 (1995). W. Kob, C. Donati, S. J. Plimpton, P. H. Poole and S. C. Glotzer, *Phys. Rev. Lett.* **79**, 2827 (1997).
- [15] K. L. Ngai and K. Y. Tsang, *Phys. Rev. E* **60**, 4511 (1999).
- [16] K. L. Ngai, *J. Phys.: Condens. Matter* **15**, S1107 (2003).
- [17] W. Götze and L. Sjögren, *Rep. Prog. Phys.* **55**, 241 (1992).